



## Deliverable 5.1. Component selection

María Arnaiz  
CICE



*Funded by the European Union. Views and opinions expressed are however those of the author(s) only and do not necessarily reflect those of the European Union or Horizon Europe. Neither the European Union nor the granting authority can be held responsible for them. No 101092080*

<b>Grant agreement Number</b>	Project 101092080 – MUSIC	
<b>Deliverable Number</b>	D5.1	
<b>Related WP</b>	WP5. Electrode development and prototype fabrication	
<b>Deliverable Title</b>	Component selection	
<b>Deliverable Date</b>	2023-06-30	
<b>Deliverable Type</b>	REPORT	
<b>Dissemination level</b>	Public (PU)	
<b>Written By</b>	María Arnaiz (CICE)	2023-06-16
<b>Checked by</b>	Jon Ajuria, Ignacio Castillo (CICE)	2023-06-18
<b>Reviewed by (if applicable)</b>	Amaia Saenz de Buruaga (BCARE)	2023-06-20
	Jørn Døvling Kaspersen (BYD)	2023-06-20
	Alberto Varzi (KIT)	2023-06-20
	Juan Pablo Badillo (ELY)	2023-06-22
	Andrea Balducci (FSU)	2023-06-26
	Thierry Brousse (IMN-CNRS)	2023-06-27
<b>Approved by</b>	Jon Ajuria (CICE)	2023-06-30
	Ignacio Castillo (CICE)	2023-06-30
<b>Status</b>	FINAL	2023-06-30

## Disclaimer / Acknowledgment



Copyright ©, all rights reserved. This document or any part thereof may not be made public or disclosed, copied or otherwise reproduced or used in any form or by any means, without prior permission in writing from the MUSIC Consortium. Neither the MUSIC Consortium nor any of its members, their officers, employees or agents shall be liable or responsible, in negligence or otherwise, for any loss, damage or expense whatever sustained by any person as a result of the use, in any manner or form, of any knowledge, information or data contained in this document, or due to any inaccuracy, omission or error therein contained.

All Intellectual Property Rights, know-how and information provided by and/or arising from this document, such as designs, documentation, as well as preparatory material in that regard, is and shall remain the exclusive property of the MUSIC Consortium and any of its members or its licensors. Nothing contained in this document shall give, or shall be construed as giving, any right, title, ownership, interest, license or any other right in or to any IP, know-how and information.

This project has received funding from the European Union's Horizon Europe programme for research and innovation under grant agreement No. 101092080. This document reflects the views of the author and does not reflect the views of the European Commission. While every effort has been made to ensure the accuracy and completeness of this document, the European Commission cannot be held responsible for errors or omissions, whatever their cause.

## Publishable summary

WP5 will focus on the design and development of sodium ion capacitors (SICs) at prototyping level to reach high energy and power densities as well as a cycle life and meet performance targets defined in WP2 for railway application. The main outcome will be the development of more sustainable and eco-friendly electrode fabrication methods based on water-based and dry processing solutions, including the final formulation of active materials, binders, and conductive additives that will be used in the pilot manufacturing line in WP6. In addition, an industrially compatible pre-sodiation strategy will be incorporated to fabricate SIC pouch cell prototypes of up to 100 F by combining selected negative and positive electrodes with the most appropriate electrolyte, to ensure compatibility and optimal interplay of all selected materials. Furthermore, the best novel active and non-active materials with regard to electrochemical capacity and capacity performance identified in WP2 and WP3 will be tested at small pouch cell prototypes for next generation of SICs. Studies of cell degradation upon cycling and endurance tests will be performed at pouch cell level. Finally, the second use of SIC will be explored by SIC regeneration and recovery of AC electrodes to build recycled EDLCs.

However, to achieve all this, first the necessity of setting up a reference system is of high importance. Hence, selecting the components that are going to serve as the baseline of the technology is necessary. This has been the work followed along Task 5.1 which is covered in this deliverable.

Thus, Generation 0 active and inactive materials have been selected to set as reference for the pouch cell assembly of WP5. Among them, hard carbon and activated carbon have been selected as the active materials for the negative and positive electrodes, respectively. Meanwhile, C45 carbon black is going to be used as conductive additive, and carboxymethyl cellulose (CMC) or its combination with styrene butadiene rubber (CMC/SBR) as binders. Moreover, disodium squarate ( $\text{Na}_2\text{C}_4\text{O}_4$ ) sacrificial salt has been selected as the Generation 0 pre-sodiation agent.

On the one hand, in order to select the most cost-effective precursor for the synthesis of the  $\text{Na}_2\text{C}_4\text{O}_4$  pre-sodiation agent, in depth study has been followed studying different squaric acid precursors. The disodium squarate obtained with each of them has been physicochemically and electrochemically characterized. The squaric acid from Apollo has been selected as the most appropriate one and at least a ratio between sacrificial salt and conductive additive of 6:1 has been demonstrated to be needed in order to ensure the complete irreversible oxidation reaction.

On the other hand, in depth study has been carried out to select the most appropriate aluminium current collector for both HC-based negative and AC-based positive electrodes. First, the validation of each slurry has been followed, continuing by their physicochemical and electrochemical characterization has been followed in bare, etched, and in two different (i.e., called ARMOR or CES) carbon coated current collectors. In regard of the validation of the slurries, HC electrodes have been fabricated using only CMC as binder and mass loadings of around  $2.5 \text{ mg cm}^{-2}$  have been achieved. In the case of the positive electrode, a rubberizer agent has been necessary to add in the formulation of the electrode in order to ensure good quality electrodes with a mass loading of around  $3.7 \text{ mg cm}^{-2}$ . Physicochemical characterization has demonstrated that both electrodes show very good properties in all the studied current collectors. However, small advantages are shown in etched and carbon coated ARMOR aluminium foils. The latter show to provide better adhesion between carbon particles and the current collector for both type of electrodes. Regarding the electrochemistry, the difference that was expected at high rates it is not visible, and all of them show very similar performance also in both type of electrodes.

Slightly difference in shown in terms of initial coulombic efficiency for the HC-based electrodes, where etched and carbon coated (ARMOR) aluminium foils show higher value.

## Contents

1	Introduction .....	8
1.1	Objective .....	8
2	Methods and Results .....	10
2.1	Generation 0 materials .....	10
2.2	Sacrificial salt precursors .....	11
2.2.1	Physicochemical characterization .....	11
2.2.2	Electrochemical characterization .....	12
2.3	Current collector selection .....	13
2.3.1	Specifications of aluminium current collectors .....	13
2.3.2	Validation of slurry formulation .....	16
2.3.3	Physicochemical characterization .....	20
2.3.4	Electrochemical characterization .....	22
3	Discussion and Conclusions .....	26
4	Recommendation .....	27
5	Risk register .....	28
6	References .....	29
7	Acknowledgement .....	30

## List of Figures

<b>Figure 1.</b> XRD patterns of Na <sub>2</sub> C <sub>4</sub> O <sub>4</sub> synthesized with different squaric acids.....	11
<b>Figure 2.</b> SEM images of disodium squarate synthesized with different squaric acids: a) Merck, b) Apollo, and c) TCI.....	12
<b>Figure 3.</b> a) Cyclic voltammetry at 0.1 mV s <sup>-1</sup> and b) Galvanostatic charge/discharge at C/10 of positive electrodes with disodium squarate synthesized with different squaric acids. ....	13
<b>Figure 4.</b> SEM images at different magnifications, and laboratory photo of different aluminium foils: a) bare from Hohsen, b) etched from Hohsen, c) carbon coated from ARMOR, and d) carbon coated from CES.....	14
<b>Figure 5.</b> Contact angle measurements for the different studied aluminium foils. <i>*Dynamic/receding contact angle due to droplet absorption by the carbon coating.</i> ....	15
<b>Figure 6.</b> Positive electrode: a) Viscosity at different shear rates, and b) mass loadings and dry thicknesses at different applied wet thicknesses when utilizing 5% of CMC binder. ....	16
<b>Figure 7.</b> Positive electrode: coatings at different wet thicknesses when utilizing 5% of CMC binder. ....	17
<b>Figure 8.</b> Positive electrode: a) Viscosity at different shear rates of CMC:SBR and CMC slurries, and b) mass loadings and dry thicknesses at different applied wet thicknesses of CMC:SBR slurry. ....	18
<b>Figure 9.</b> Positive electrode: coatings in the different studied current collectors and their mass loading and dry thickness. ....	18
<b>Figure 10.</b> Negative electrode: a) Viscosity at different shear rates of AC (CMC:SBR) and HC (CMC) slurries, and b) mass loadings and dry thicknesses at different applied wet thicknesses of HC (CMC) electrodes. ....	19
<b>Figure 11.</b> Negative electrode: coatings at different wet thicknesses. ....	19
<b>Figure 12.</b> Negative electrode: coatings in the different studied current collectors and their mass loading and dry thickness. ....	20
<b>Figure 13.</b> Positive electrode: SEM cross-sectional images on the different studied current collectors. ....	20
<b>Figure 14.</b> Negative electrode: SEM cross-sectional images on the different studied current collectors. ....	21
<b>Figure 15.</b> Positive electrode: 90° adhesion tests of the coatings made in different current collectors. ....	22
<b>Figure 16.</b> 90° adhesion tests of the negative electrodes made in different current collectors: a) strength required, b) lab photos of the samples. ....	22
<b>Figure 17.</b> Cyclic voltammeteries for the positive electrodes fabricated in different aluminium foils: a) etched from Hohsen, b) carbon coated from ARMOR, c) carbon coated from CES, and comparison between them at d) 20 mV s <sup>-1</sup> and e) 100 mV s <sup>-1</sup> .....	23
<b>Figure 18.</b> Galvanostatic charge/discharge measurements of the positive electrode with different aluminium foils: a) Specific capacitance output, and b) Profiles at 7 A g <sup>-1</sup> . ....	24
<b>Figure 19.</b> Cyclic voltammeteries for the negative electrodes fabricated in different aluminium foils: a) 1 <sup>st</sup> cycle, and b) 10 <sup>th</sup> cycle both at 1 mV s <sup>-1</sup> .....	24
<b>Figure 20.</b> Galvanostatic charge discharge of the negative electrode in different current collectors: a) First charge/discharge profiles, and b) Rate capability.....	25

## List of Tables

<b>Table 1.</b> Information about different selected squaric acids. ....	11
<b>Table 2.</b> Information about under study aluminium current collectors.....	14
<b>Table 3.</b> Materials, formulation, and cell composites for Gen0 positive and negative electrodes.....	16
<b>Table 4.</b> Risk Register.....	28
<b>Table 5.</b> Project partners.....	30

## List of Equations

No entries for the list of equations found.

## Abbreviations

SYMBOL	SHORTNAME
AC	Activated Carbon
Al	Aluminium
CMC	Carboxymethylcellulose
CRM	Critical Raw Material
CV	Cyclic Voltammetry
CE	Coulombic efficiency
EC	Ethylene Carbonate
Gen0	Generation 0
GCPL	Galvanostatic Cycling with Potential Limitation
HC	Hard Carbon
NMP	N-methyl-2-pyrrolidone
PC	Propylene Carbonate
PTFE	Polytetrafluoroethylene
PVdF	Polyvinylidene difluoride
RT	Room Temperature
PSD	Pore Size Distribution
SSA	Specific Surface Area
SEI	Solid Electrolyte Interphase
SEM	Scanning-electron microscopy
SIC	Sodium Ion Capacitor
WP	Work Package
XRD	X-ray diffraction

# 1 Introduction

## 1.1 Objective

The aim of this Deliverable is to select the components that are going to be utilized in the fabrication of sodium ion capacitor (SIC) prototypes. Among those, active and inactive materials set as Generation 0 for WP3-4-5 are selected. Moreover, special focus has been put on the selection of the current collector.

The abundance of sodium and the absence of costly transition metals in electrodes are the significant strongholds why MUSIC aims at developing dual carbon SICs. Carbonaceous **negative electrode** materials play a key role in achieving high energy-power performance SICs. Generally, suitable anode materials for SICs need to possess high capacity at low potential voltage window ( $<1.0$  V vs.  $\text{Na}^+/\text{Na}$ ) and excellent rate capability, as well as superior cycling stability. Excluding graphite owing to its classification as a Critical Raw Material (CRM) and benefiting from low cost ( $<50$  €  $\text{kg}^{-1}$ ), sustainability, and good physical/chemical stability, a series of carbonaceous materials such as hard carbon (HC), soft carbon, heteroatom-doped carbon, and carbon composites are vastly studied for sodium ion technology.[1] Regarding the **positive electrodes** for SICs, despite several carbonaceous materials have been studied (e.g., graphene, carbon nanotubes or aerogels), most widely used capacitor-type electrodes are fabricated with an activated carbon (AC) that possesses very large specific surface area (SSA) and narrow pore size distribution (PSD) to enhance the power density, which is promoted via surface charge-storage processes. ACs are low-cost ( $< 40$  €  $\text{kg}^{-1}$ ), present adaptable porous texture, high SSA ( $1500\text{--}2000$   $\text{m}^2$   $\text{g}^{-1}$ ), good chemical stability, and high conductivity ( $60$  S  $\text{cm}^{-1}$ ).[2] The addition of a **conductive additive** is also necessary in order to ensure electronic conductivity. Among the most utilized ones, different carbon blacks, carbon nanotubes, or graphites are employed. The charge storage capability of these materials normally is quite low. However, depending on the selected material, it should also be considered.

Considering that MUSIC targets dual carbon SICs, the lack of an inherent source of internal ions elevates **pre-sodiation** to an unprecedented technological challenge. Moreover, an accurate pre-sodiation step will allow to sodiate the negative electrode in its most appropriate degree, enlarge the potential window of the positive electrode, and increase the cell voltage. Therefore, a precise pre-sodiation step will result not only in a higher energy density output, but also in improved power performance as well as longer cycle life.

Furthermore, in order to realize high power devices, it is necessary to design **electrolytes** with good transport properties, able to support the fast ion mobilities required to sustain the high current densities which are typically applied in these systems. Furthermore, the electrolyte needs to display large electrochemical stability as well as high thermal and chemical stabilities. These latter properties are needed to guarantee high operative voltage, high cycling stability and broad temperature range of use for the devices in which they are used. [3]

Fluorinated thermoplastic polymers such as polytetrafluoroethylene (PTFE) and polyvinylidene difluoride (PVdF) are the state-of-the-art **binders** used for fabricating battery and capacitors electrodes. Besides the environmental concerns associated with fluorine containing compounds (from synthesis to disposal/recycling), more importantly, the binder determines the solvent of choice for electrode preparation. While PTFE can be dispersed in water, PVdF requires the use of expensive and toxic organic solvents, such as N-methyl-2-pyrrolidone (NMP) which is a teratogenic and irritating compound. For this reason and the economic impact, many efforts have been made to develop fluorine-free binders that can be easily processed in water. Carboxymethylcellulose (CMC) is the most popular aqueous binder, but its major disadvantage is that mass loading achievable is



limited, the reason being the shrinkage of CMC chains during drying which can lead to cracking of the coating.[4,5]

Sodium ion technology allows the use of aluminium **current collector** in both negative and positive electrodes. However, being SICs a high-power technology, special attention should be taken on the selection of the current collector in order to reduce the resistance and enhance the energy efficiency of the devices. Thus, etched or carbon coating treated aluminium foils have been shown to be appropriate for this purpose.

At the same time, it is also needed a **separator** that ensures fast ion transport. In this regard, polymeric or cellulose based separators are normally considered. While the **case** utilized for **pouch cell** assembly is always a heat resistant polymeric one. The material for **tabs** depends on the nature of the current collector, being aluminium foil for SICs, tabs can be of the same material.[6,7]

## 2 Methods and Results

### 2.1 Generation 0 materials

The selection of the components for SICs assembly in this WP started by setting the Generation 0 (Gen0) active and inactive materials for electrode fabrication. In all cases, commercially available materials have been selected for benchmarking.

Among the different carbonaceous materials possible to use as anode material, graphite is discarded due to its instability with carbonate solvents of the electrolyte, while, to the best of our knowledge, no commercially available soft carbons are available capable of meeting the required performance targets. Thus, as several commercially available hard carbons (HCs) can be found in the market, it has been selected as the active material for the negative electrode. HC has been purchased from Kuraray, one of the first companies commercializing HCs, with a wide portfolio of specific HCs, even specifically designed for water processing, one of the major goals of the MUSIC project. [8] Regarding the positive electrode, YP-50F activated carbon also from Kuraray is selected. This material shows high SSA (*i.e.*,  $1700 \text{ m}^2 \text{ g}^{-1}$ ) appropriate for SICs technology. [9] However, along the project the up-scaled sawdust derived super activated carbon from BYD will be introduced for WP5 prototypes.

The pre-sodiation agent selected as Gen0 material is disodium squarate ( $\text{Na}_2\text{C}_4\text{O}_4$ ) sacrificial salt, which has already been validated in SICs technology by some partners of MUSIC project.[10] This sacrificial salt shows high irreversibility of  $339 \text{ mAh g}^{-1}$  at around  $3.6 \text{ V vs. Na}^+/\text{Na}$ , is air-stable, can be processed in atmospheric conditions, and the only products generated by its oxidation are CO and  $\text{CO}_2$  gas that can be eliminated after the pre-conditioning step. Thus, it shows to be suitable to be set as Gen0 pre-sodiation agent. Disodium squarate synthesis employs  $\text{Na}_2\text{CO}_3$  and squaric acid precursors. The latter suffered a high price increase during the last years, obeying the search for a cost-effective alternative provider. This will be evaluated in [Section 2.2](#) of this D5.1.

In order to ensure the electronic conductivity of the fabricated electrodes, C-ENERGY™ SUPER C45 is introduced as conductive additive, as it shows to be the most appropriate commercial conductive additive for aqueous processing [11], while as binder, the most utilized sodium carboxymethylcellulose (CMC) is selected.

The formulation to fabricate the hard carbon negative electrodes is set on utilizing 90 wt.% of HC, 5 wt.% of C45 wt.% and 5 wt.% of CMC. Whereas for the positive electrodes, 5 wt.% of C45 and 5 wt.% of binder is kept, while the percentage of the activated carbon would vary depending on the sacrificial salt wt.% required. Thus, the amount of active material is defined as  $(90-x) \%$ , being  $x$  the percentage of the sacrificial salt. The current collector where the above-mentioned slurries are coated deserves a special analysis, which is carried out in [Section 2.3](#) of this D5.1.

In terms of electrolyte selection, an important point is its ability to promote the formation of stable interfaces, *e.g.*, the solid electrolyte interphase (SEI), which is needed for the realization of highly reversible and prolonged storage processes. So far, most of the electrolytes which have been utilized in SICs have been based on mixtures of carbonates, *e.g.*, ethylene carbonate (EC) and propylene carbonate (PC), and a sodium salt, mainly sodium fluorophosphate ( $\text{NaPF}_6$ ). This electrolyte displays good transport properties and allows the realization of high voltage SICs. Thus, 1M  $\text{NaPF}_6$  in a mixture of ethylene carbonate and propylene carbonate in a ratio of 50:50 v/v, provided by E-lyte (ELY partner), has been selected as the benchmark electrolyte utilized in sodium energy storage technology.

While among inactive components, cellulose separator that allows fast ion transport has been selected when assembling pouch cell prototypes, polymeric cell casing and aluminium tabs.

## 2.2 Sacrificial salt precursors

As mentioned in previous section, the only drawback of the disodium squarate ( $\text{Na}_2\text{C}_4\text{O}_4$ ) sacrificial salt selected as Gen0 pre-sodiation agent comes from the cost of one of its precursors, *i.e.*, the squaric acid. Thus, a specific analysis of different squaric acids has been followed in Task 5.1 in order to select the most appropriate one in terms of performance and cost. **Table 1** describes the three different squaric acids that have been analysed.

**Table 1.** Information about different selected squaric acids.

Provider	Product reference	Description	Unitary price (€)
Merck	123447-25g	3,4-Dihydroxy-3-cyclobutene-1,2-dione $\geq 99.0\%$ (HPLC)	220,00
Apollo	54-OR28821-25g	3,4-Dihydroxycyclobut-3-ene-1,2-dione, $>99,7\%$ (HPCL)	64,00
TCI	3B-D1399-25g	3,4-Dihydroxy-2-cyclobutene-1,2-dione, $>98\%$ (HPCL)	133,00

### 2.2.1 Physicochemical characterization

Disodium squarate ( $\text{Na}_2\text{C}_4\text{O}_4$ ) is synthesized using 3,4-dihydroxy-3-cyclobutene-1,2-dione (squaric acid) and  $\text{Na}_2\text{CO}_3$  as starting materials. Within a 1:1 molar stoichiometric relation, each precursor is dissolved in the required deionized water. Once both are well-dissolved,  $\text{Na}_2\text{CO}_3$  solution is added slowly into the one of the squaric acid and stirred. Then, the deionized water is removed by using a rotavapor and the obtained sodium salt is dried under vacuum at  $60^\circ\text{C}$  for 12 hours. This procedure has been followed with the different squaric acids defined in Table 1. **Figure 1** describes the X-Ray Diffraction (XRD) pattern of each of them in comparison with the XRD pattern from the ICDS database. As it is shown, the  $\text{Na}_2\text{C}_4\text{O}_4$  material is successfully obtained with all the studied precursors.

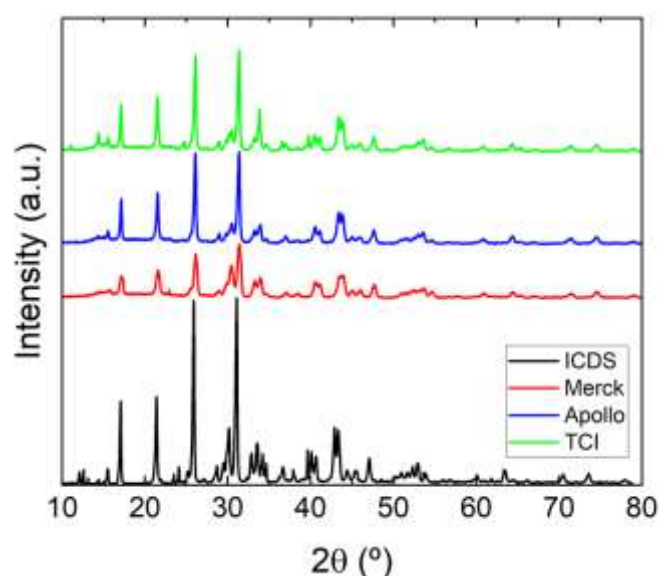


**Figure 1.** XRD patterns of  $\text{Na}_2\text{C}_4\text{O}_4$  synthesized with different squaric acids.

In order to evaluate the electrochemical response of the three different sacrificial salts, positive electrodes with a formulation of AC:Na<sub>2</sub>C<sub>4</sub>O<sub>4</sub>:C65:PVdF in weight ratio of 50:40:5:5 have been fabricated coated in aluminium foil. As conductive additive, C65 is preferred for organic processing whereas C45 will be selected when processing in water. It is expected that the aqueous processing of the positive electrode within the sacrificial salt could present new challenges that would deserve in depth research. Thus, as the main purpose of this study is to select the best precursor for the sacrificial salt, the electrode processing has been followed in NMP organic solvent. However, the development of the positive electrode aqueous processing together with the sacrificial salt will be followed in next Task 5.2 (*i.e.*, Positive electrode processing).

Before slurry formulation, the sacrificial salt and conductive additive are dry-mixed utilizing ball milling method. This step allows to ensure an appropriate carbon coating of the pre-sodiation agent. **Figure 2** shows Scanning Electron Microscope (SEM) images of the different materials. In all of them few agglomerates that later are expected to be destroyed during the mixing process are observed.

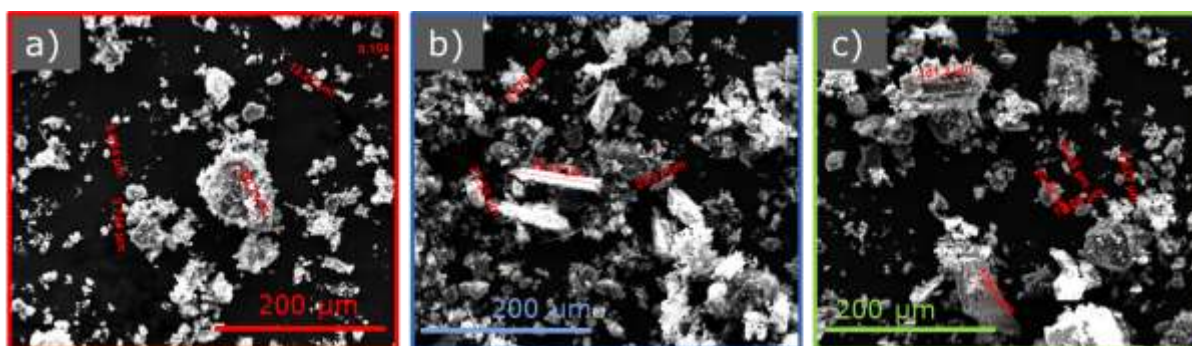


**Figure 2.** SEM images of disodium squarate synthesized with different squaric acids: a) Merck, b) Apollo, and c) TCI.

### 2.2.2 Electrochemical characterization

The electrodes fabricated using above-mentioned method were electrochemically characterized in three electrode Swagelok cells utilizing an oversized activated carbon as counter electrode, sodium metal as reference electrode, all immersed in 1M NaPF<sub>6</sub> (EC:PC) electrolyte. Cyclic voltammetry (CV) at 0.1 mV s<sup>-1</sup> and galvanostatic charge/discharge measurements at C/10 (being C = 339 mAh g<sup>-1</sup>) have been followed for all samples between 2 – 4.2 V vs. Na<sup>+</sup>/Na (see **Figure 3**). **Figure 3a** shows the CV for each sample where the sacrificial salt is carbon coated in a ratio of 8:1 (in the overall formulation as 40:10), but also with a 6:1 ratio (in the overall formulation as 30:10). Same as in **Figure 3b**, showing the capacity output of the first charge/discharge cycle. The Na<sub>2</sub>C<sub>4</sub>O<sub>4</sub>:C65 ratio was reconsidered due to the displacement and broad peak observed in CV results, and sloppy profile in galvanostatic charge/discharge when describing the oxidation of the sacrificial salt.

Since the XRD pattern and the electrochemical response among the different Na<sub>2</sub>C<sub>4</sub>O<sub>4</sub> is not showing significant difference among them, the squaric acid from Apollo, which is the cheapest and the purest one, is selected as the precursor to be used in the Na<sub>2</sub>C<sub>4</sub>O<sub>4</sub> preparation. Thus, the electrodes with the new AC:Na<sub>2</sub>C<sub>4</sub>O<sub>4</sub>:C65:PVdF ratio of 60:30:5:5 are already fabricated with the disodium squarate prepared with the squaric acid from Apollo. The new Na<sub>2</sub>C<sub>4</sub>O<sub>4</sub>:C65 ratio, with a higher amount of conductive additive, shows remarkable improvements in CV and GPCL measurements. In Figure 3a a clear and sharp peak at around 3.6 V vs. Na<sup>+</sup>/Na describes the complete oxidation reaction of the sacrificial salt, while in Figure 3b, the polarization of the oxidation reaction has been decreased

showing a much more appropriate plateau at around 3.6 V vs. Na<sup>+</sup>/Na. Moreover, capacity output has been enlarged, and is closer to the theoretical one.

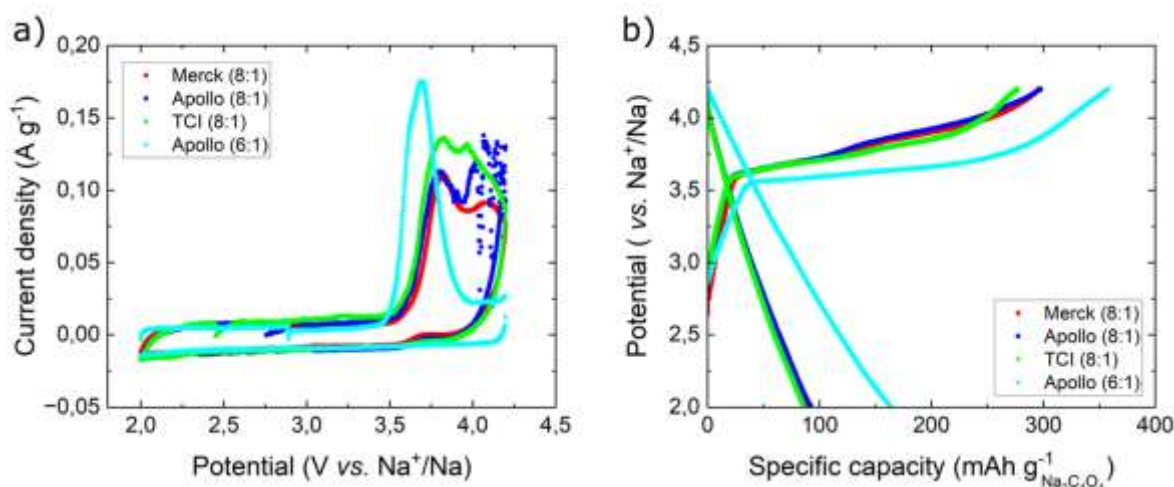


**Figure 3.** a) Cyclic voltammetry at 0.1 mV s<sup>-1</sup> and b) Galvanostatic charge/discharge at C/10 of positive electrodes with disodium squarate synthesized with different squaric acids.

Thus, physicochemical and electrochemical results allow us to conclude that the squaric acid from Apollo can be utilized as a cost-effective precursor for disodium squarate pre-sodiation agent preparation.

## 2.3 Current collector selection

The current collector selection is of key importance when working with high-power devices. The contact between the coating and current collector must be enhanced in order to reduce the contact resistance and enhance the electron transportation. The strategies followed to reduce it focuses on selecting an etched or carbon coating current collector. As any technology based on Na-ion chemistry, SICs develop in this project allows to use aluminium foil in both positive and negative electrodes, as alloying reactions are not taking place within the operational voltage window.

### 2.3.1 Specifications of aluminium current collectors

The study to select the most appropriate current collector has been focused on three different aluminium foils (see **Table 2**), having as reference an aluminium foil without any treatment (*i.e.*, bare). The current collectors have been selected owing to their specific properties. Contact with more companies was followed but also discarded due to high cost, lack of specifications, or missing response. The studied aluminium foils have been purchased to Hohsen, ARMOR, and CES companies.

**Table 2.** Information about under study aluminium current collectors.

Properties Aluminium foil	Bare (Hohsen)	Etched (Hohsen)	C-coated (ARMOR)	C-coated (CES)
Mass loading (mg cm <sup>-2</sup> )	5.31	5.08	4.18	4.05
Thickness (µm)	20	20	15	12
Density (g cm <sup>-3</sup> )	2.65	2.54	2.77	3.37
Price (€/m <sup>2</sup> )	8.0	24.0	11.41	5.83
Origin	Asia	Asia	Europe	Europe

The microstructural analysis of the different current collectors is followed by SEM. **Figure 4** shows the surface SEM images at different magnifications (left) and pictures taken in the lab for each aluminium foil (right). **Figure 4a** describes bare aluminium foil from Hohsen company, while **Figure 4b** the etched one, which at high magnifications is clearly possible to see the rugous surface that allows the slurry to better penetrate and ensure contact. **Figure 4c** shows the 1 µm carbon coated aluminium foil from ARMOR company. Not only visually, but SEM images also confirm that a full covered carbon coating can be found in the surface of the aluminium. Similar to the etched one, in this case, the slurry would penetrate along the carbon coating and ensure an optimum contact between the coated slurry and current collector. The fourth studied aluminium foil is also a carbon coated one, however, visually it already shows big differences with the previous one (see **Figure 4d**). The visual inspection of the carbon-coated aluminium foil from CES company shows not a complete coating, but some lines where the aluminium can be observed are visible. SEM images reveal a heterogeneous coating of carbon nanoparticles.

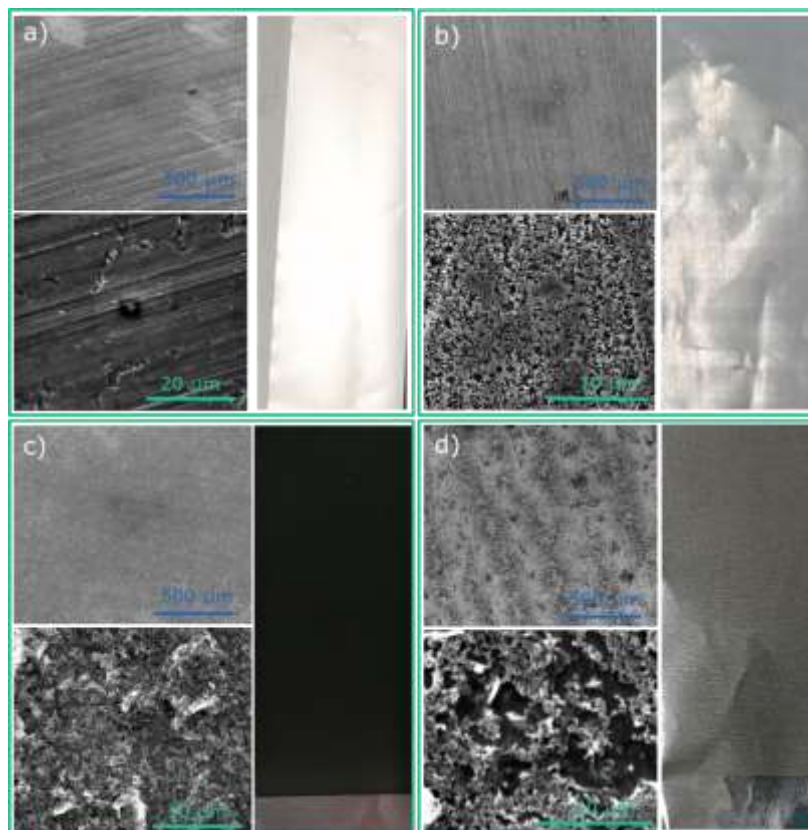


**Figure 4.** SEM images at different magnifications, and laboratory photo of different aluminium foils: a) bare from Hohsen, b) etched from Hohsen, c) carbon coated from ARMOR, and d) carbon coated from CES.

Moreover, the hydrophobicity of the different aluminium foils is studied by measuring the contact angle. This measurement reflects the wettability of the slurry with the current collector, which affects the electron transport inside the system. **Figure 5** reveals that the aluminium foil with highest contact angle and hence, the one with higher hydrophobicity, is the bare (not etched, not carbon coated) aluminium foil. While, etched and CES carbon coated aluminium foils show similar contact angle of around 20°. The carbon coated aluminium foil from ARMOR shows similar value as soon as it is wet. However, the drop is completely dispersed in the foil after few seconds, showing its total hydrophilicity. Thus, contact angle results allow us to expect better wettability of aqueous-based slurries in etched and carbon coating aluminium foils.

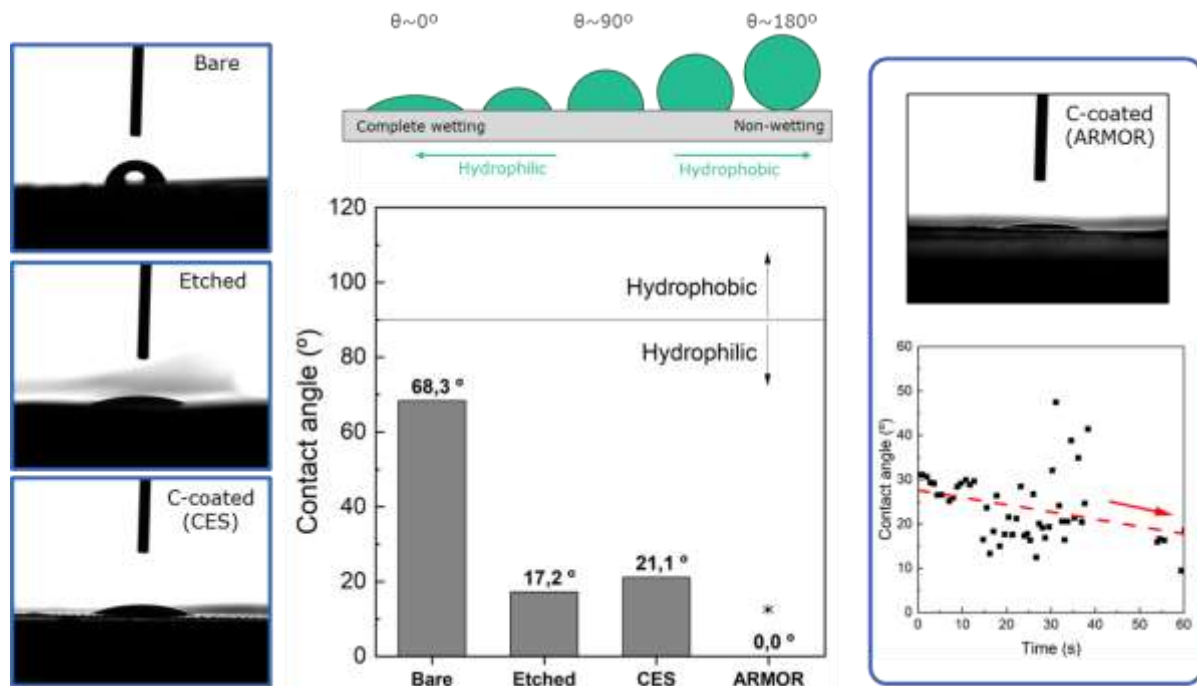


**Figure 5.** Contact angle measurements for the different studied aluminium foils. \*Dynamic/receding contact angle due to droplet absorption by the carbon coating.

In order to validate the selected current collectors in both positive and negative electrodes, the slurry formulation and cell characteristics have been previously defined. **Table 3** briefly describes the slurry formulation, the mass loadings that are aimed to obtain, and the electrolyte and separator that are going to be utilized for the cell assembly. In the current study the sacrificial salt is not introduced in the formulation of the positive electrode to make the analysis simpler. The ahead Task 5.2. would cover that development.

**Table 3.** Materials, formulation, and cell composites for Gen0 positive and negative electrodes.

	Positive electrode	Negative electrode
Active material (AM)	Activated Carbon ( <i>YP-50F, Kuraray</i> )	Hard Carbon ( <i>Kuraray</i> )
Conductive additive (CA)	Carbon Black ( <i>C-ENERGY 45, IMERYS</i> )	Carbon Black ( <i>C-ENERGY 45, IMERYS</i> )
Binder (B)	CMC ( <i>DS: 0.7; MW=250000</i> )	CMC ( <i>DS: 0.7; MW=250000</i> )
Formulation (AM:CA:B)	90:5:5	90:5:5
Current collector	Aluminium foil	Aluminium foil
Mass loading	2.5-5 mg cm <sup>-2</sup>	2-3 mg cm <sup>-2</sup>
Electrolyte	1M NaPF <sub>6</sub> EC:PC	1M NaPF <sub>6</sub> EC:PC
Separator	Glass fiber D (lab-scale)	Glass fiber D (lab-scale)

Thus, in order to evaluate the influence of using one or other aluminium foil, first of all, a good processing of the slurry has to be ensured, to secondly, being able to characterize physiochemically and electrochemically good quality electrodes.

### 2.3.2 Validation of slurry formulation

The validation of the slurry formulation comes by analysing the rheological properties of the slurry, the presence or not of agglomerates, and the coating and drying behaviour, among others.

Initially the positive electrode is formulated utilizing activated carbon (AC) as active material in a 90 wt.%, with 5 wt.% of C45 as conductive additive, and 5 wt.% CMC as binder. The slurry is initiated by preparing the binder solution in distilled water, then, C45 is added, and after the proper mixing speed and time, AC is introduced and dispersed. The solid content of AC nature slurries is around 30%. Once, all components have been homogeneously dispersed, the rheological properties of the slurry are analysed. **Figure 6a** shows the variable viscosity while stressing the slurry at different shear rates describing a non-Newtonian fluid. Moreover, the decrease of the later with the increase of the shear strain shows a shear thinning behaviour fluid. This is typical and desired behaviour for electrode coatings. **Figure 6b** shows the mass loading and dry thicknesses of the electrodes fabricated with above-described slurry.

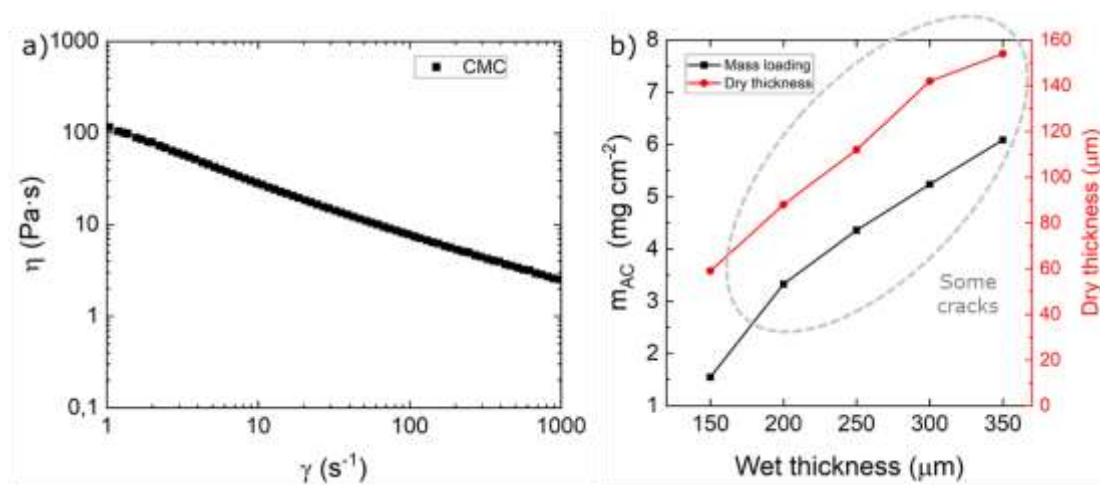


**Figure 6.** Positive electrode: a) Viscosity at different shear rates, and b) mass loadings and dry thicknesses at different applied wet thicknesses when utilizing 5% of CMC binder.



The target mass loading would be between the wet thickness of 200 and 250  $\mu\text{m}$ . However, **Figure 7** reveals that on those coatings, some cracks are easily obtained as soon as the coating is dried at Room Temperature (RT) for 2 hours. Moreover, following the drying step at 80°C overnight, the cracks are worsened due to the CMC shrinkage. Thus, these results show the necessity of introducing a rubberizer agent on the slurry formulation capable to keep the integrity of the electrodes on the targeted mass loadings.

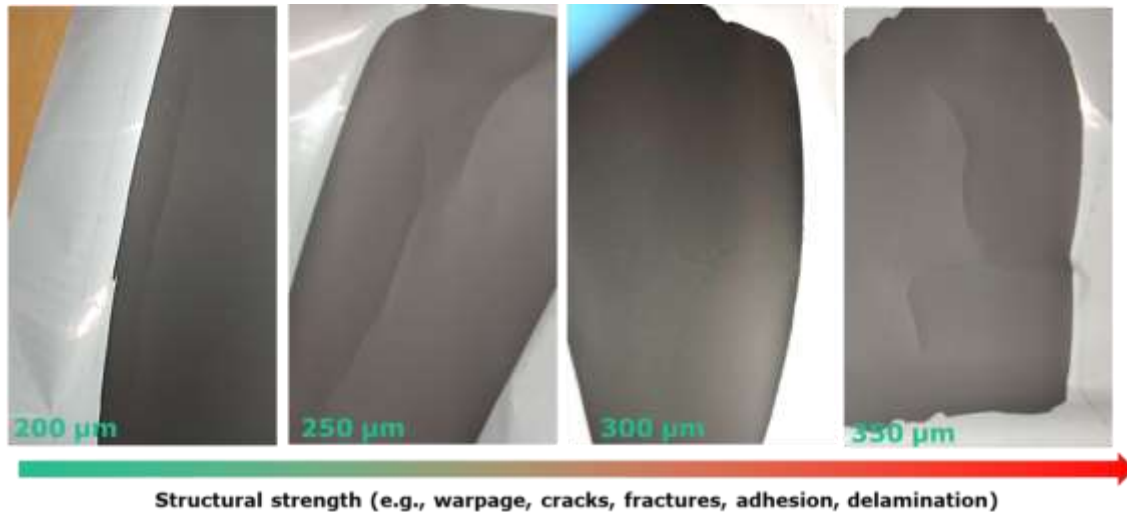


**Figure 7.** Positive electrode: coatings at different wet thicknesses when utilizing 5% of CMC binder.

Within that goal, the formulation of the AC positive electrode is changed to 90 wt.% AC, 5 wt.% of C45, and 3 wt.% of CMC together with 2 wt.% SBR. **Figure 8a** shows the viscosity along different shear rate of the new formulation in comparison with the only CMC one. As it is observed, it also shows a non-Newtonian and shear thinning behaviour, but with lower viscosity values. This is directly related with the lower CMC content and with the factor that the solid-liquid relation has been kept constant in order not to introduce more variables on the study. Hence, the reduction of 2 wt.% in the formulation is the main responsible of the viscosity reduction. However, the better properties in terms of particle cohesion due to the stronger polymer chains of SBR allows to obtain the desired mass loadings of around  $3.5 \text{ mg cm}^{-2}$  without showing any crack along the coating. The aim would be to achieve up to  $5 \text{ mg cm}^{-2}$  electrodes, however,  $3.5 \text{ mg cm}^{-2}$  has been stabilized as Gen0 maximum mass loading achievable with Gen0 binders.

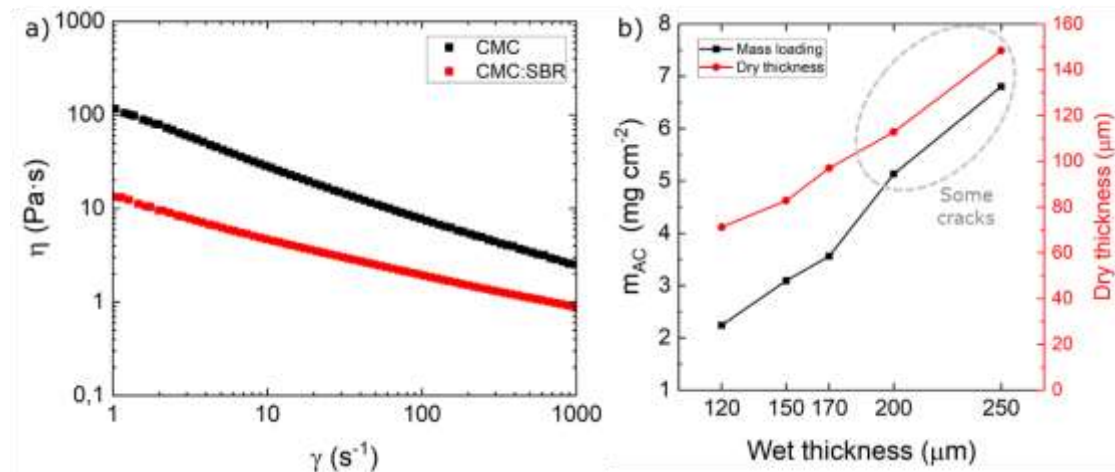


**Figure 8.** Positive electrode: a) Viscosity at different shear rates of CMC:SBR and CMC slurries, and b) mass loadings and dry thicknesses at different applied wet thicknesses of CMC:SBR slurry.

**Figure 9** shows the photos of the coatings made with 150  $\mu m$  wet thickness and the mass loading values of around 3.5  $mg\ cm^{-2}$  and 80  $\mu m$  for each different aluminium foil. Bare aluminium foil has not been considered for the study on the positive electrode as from previously studies the importance of using a surface treated current collector has been reported. [6]

These electrodes are the ones physicochemically characterized in [Section 2.3.3](#), and electrochemically characterized in [Section 2.3.4](#).

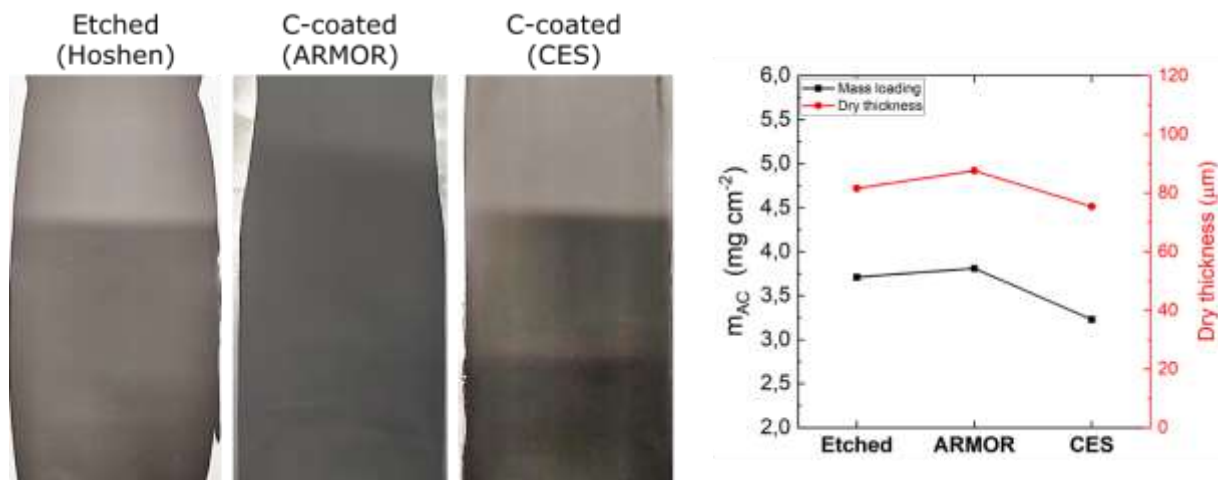


**Figure 9.** Positive electrode: coatings in the different studied current collectors and their mass loading and dry thickness.

Regarding the negative electrode, and going back to Table 3, it has been formulated by utilizing hard carbon (HC) as active material in a 90 wt.%, with 5 wt.% of C45 as conductive additive, and 5 wt.% CMC as binder. Same as for the positive electrode, the slurry formulation of the HC is started by preparing the binder solution in distilled water, then, C45 is added, and after the proper mixing speed and time, HC is introduced and dispersed. The solid content of HC nature slurries would be around 40%, as the higher density and lower porosity of the material does not require as much liquid content as it is required for the positive electrode. Once, all components have been homogeneously dispersed, the rheological properties of the slurry are analysed. **Figure 10a** shows the

comparison between the Gen0 slurry for the positive electrode (*i.e.*, utilizing 3wt.% CMC and 2 wt.% SBR as binder), and the HC-based one. As observed, it presents same similar non-Newtonian and shear thinning behaviour. Moreover, the viscosity values along the different studied shear rates show to be quite similar. However, owing to the different nature of the carbons, for the HC slurry, lower wet thickness values are possible to apply to obtain similar mass loadings (see **Figure 10b**).

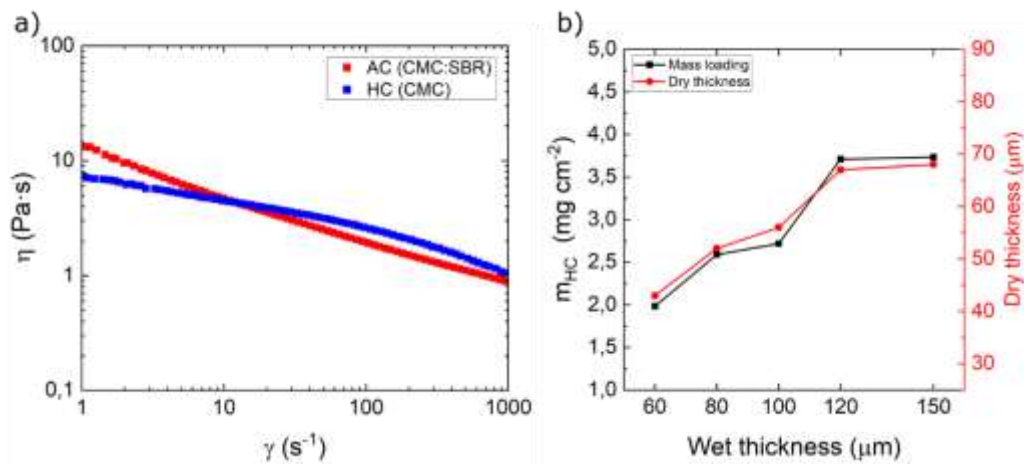


**Figure 10.** Negative electrode: a) Viscosity at different shear rates of AC (CMC:SBR) and HC (CMC) slurries, and b) mass loadings and dry thicknesses at different applied wet thicknesses of HC (CMC) electrodes.

In the case of the negative electrodes - with only CMC- there is absence of cracks up to the highest mass loading of 3.7 mg cm<sup>-2</sup>, where only some cracks are formed when handling the laminates.

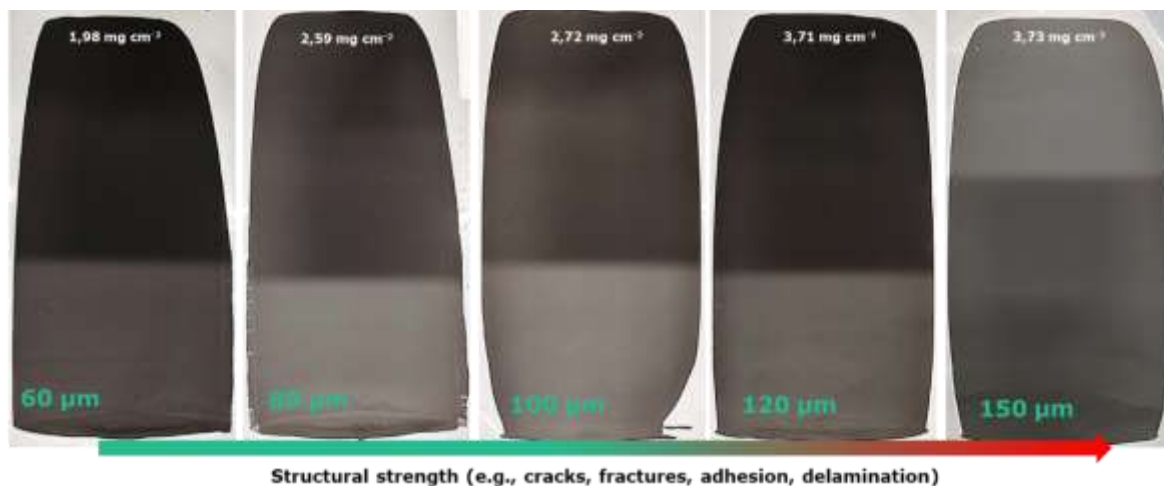


**Figure 11.** Negative electrode: coatings at different wet thicknesses.

Thus, the wet thickness of 80 μm has been selected to fabricate HC electrodes in the different studied aluminium foils. **Figure 12** shows the pictures of the coatings and the mass loading and dry thickness values for each of them, which are around 2.5 mg cm<sup>-2</sup> and 40 μm. These electrodes are the ones physiochemically characterized in [Section 2.3.3](#), and electrochemically characterized in [Section 2.3.4](#).

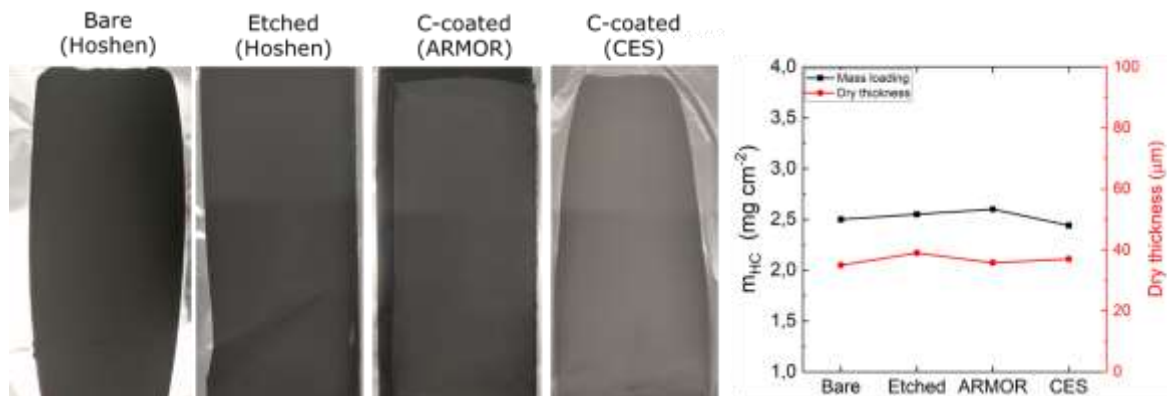


**Figure 12.** Negative electrode: coatings in the different studied current collectors and their mass loading and dry thickness.

### 2.3.3 Physicochemical characterization

The physicochemical characterization of the fabricated positive and negative electrode allows to determine the quality of the fabricated electrodes. SEM microstructural analysis describes if a good dispersion of the different materials is achieved, while the contact between the coatings and the aluminium foils (*i.e.*, adhesion) and the contact among particles (*i.e.*, cohesion) is analysed by cross-sectional SEM images and 90° adhesion tests.

On the one hand, **Figure 13** describes the cross-sectional SEM images of the coatings of the positive electrode (Figure 9). As it can be observed, homogeneous distribution of materials is obtained, while perfect adhesion of particles and aluminium foil is achieved. In the etched aluminium foil, some rugosity can be observed at the highest magnification picture. On the contrary, a clear continuous 1  $\mu\text{m}$  carbon coating is observed in the ARMOR one, which is perfectly ensuring the contact among particles and current collector. Finally, the CES carbon coated aluminium foil shows a coating that seems to be inhomogeneous, however, the particles and current collector contact shows to be also quite good. Thus, overall, all coatings show good cohesion and adhesion.

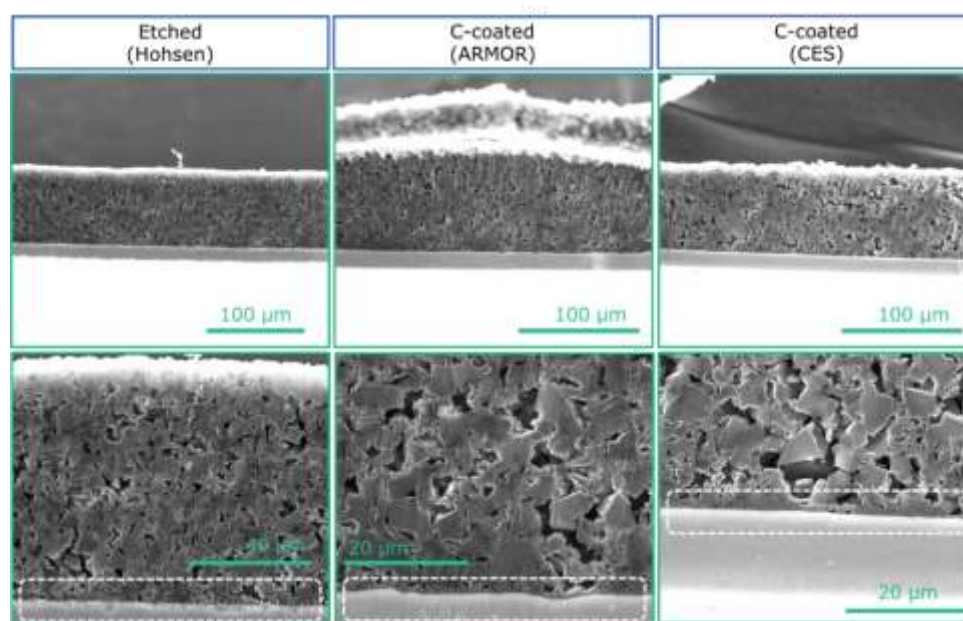


**Figure 13.** Positive electrode: SEM cross-sectional images on the different studied current collectors.

On the other hand, **Figure 14** describes the cross-sectional SEM images of the coatings of the negative electrode (Figure 12). In this case, as previously measured, and owing to the nature of the material, it is shown that the thicknesses of the HC coatings are much lower than their AC counterparts even that they are of similar mass loading. In Figure 14 it can be observed that the contact, and hence, the cohesion between particles shows to be good. However, a calendaring step might still improve the contact among particles that will be beneficial for its electrochemical performance. Nevertheless, this will be studied more in detail in Task 5.3 (*i.e.*, Negative electrode processing). Regarding the adhesion, the coatings made in the bare, etched, and CES carbon coated aluminium foils seem not to be totally homogeneous, despite this, they show to be of enough quality. In the case of ARMOR carbon coated HC electrode, the contact between particles together with the current collector shows to higher quality.

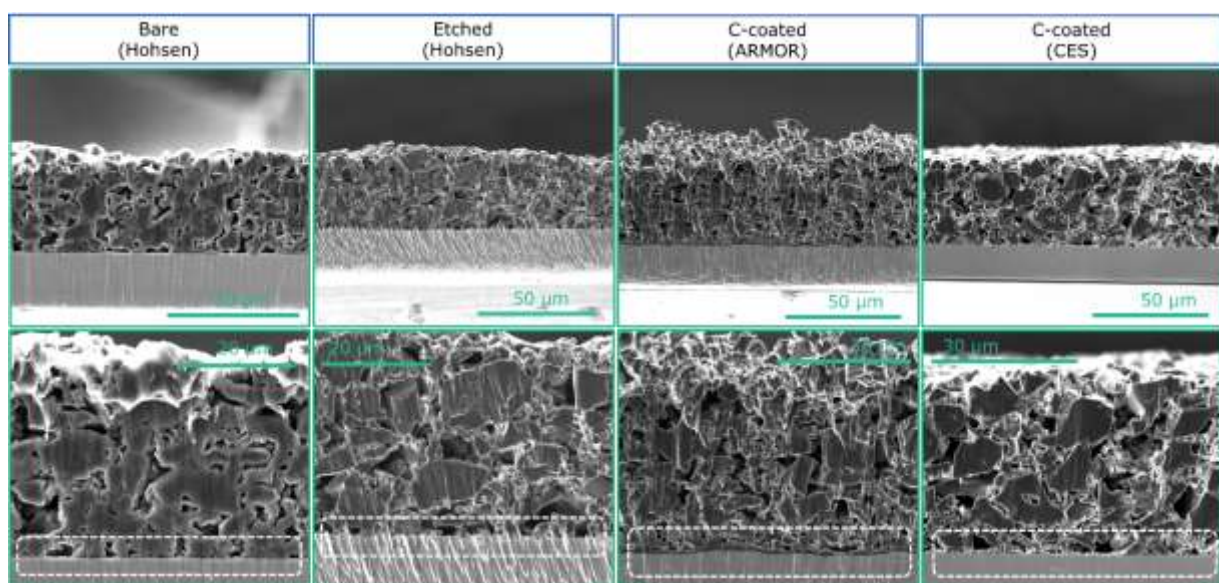


**Figure 14.** Negative electrode: SEM cross-sectional images on the different studied current collectors.

The adhesion quality of the coatings with the current collector is also evaluated by 90° adhesion tests. **Figure 15a** shows that a similar force needs to be applied to each of the coatings, what means that they show similar cohesive/adhesive properties. **Figure 15b** shows some pictures taken in the laboratory, describing the material that the tape has removed along the measurement. Even though force values are very similar, it seems that slightly more carbon is removed in the CES coating, describing slightly worst cohesion among particles.

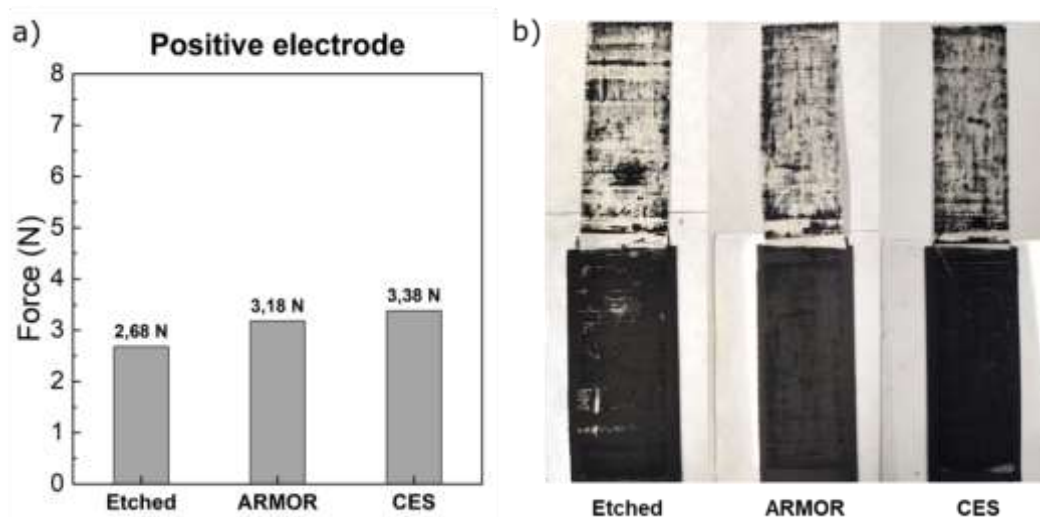


**Figure 15.** Positive electrode: 90° adhesion tests of the coatings made in different current collectors.

In the case of the negative electrode, in **Figure 16a** all of them show higher adhesion forces, describing better quality than their AC counterparts. This is directly related to the lower porosity and higher density of the active material, the higher solid content of the slurry, and consequently, its better drying behaviour. **Figure 16b** shows some pictures taken in the laboratory, describing the material that the tape has removed along the measurement. No clear difference can be evidenced.

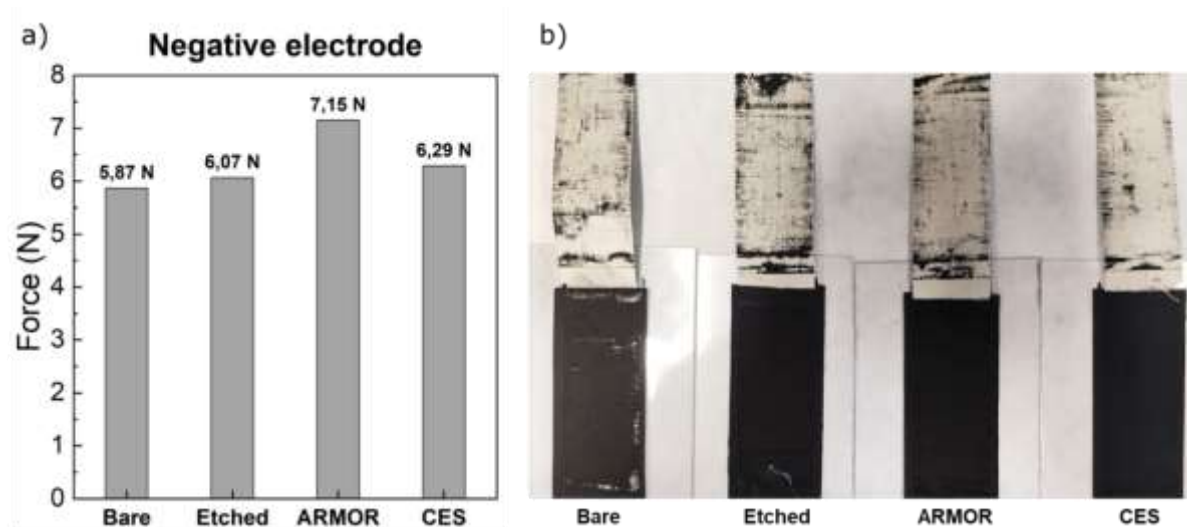


**Figure 16.** 90° adhesion tests of the negative electrodes made in different current collectors: a) strength required, b) lab photos of the samples.

Overall, the 90° adhesion tests for both positive and negative electrodes in different current collectors show that Gen0 electrodes of high quality have been fabricated.

### 2.3.4 Electrochemical characterization

Electrochemical characterization of the fabricated electrodes might give some insights on the resistance that each aluminium foil can provide to the fabricated positive and negative electrodes. In order to evaluate their performance in the different studied aluminium current collectors, cyclic voltammetry (CV), and galvanostatic charge/discharge

measurements have been followed. These measurements allow to evaluate the possible resistance increase with the increase of the applied scan-rate/current. Hence, to give some insights in which type of electrode shows the highest contact resistance between the coating and current collector. Electrochemical measurements have been carried out in three electrode cells using in all the cases sodium metal as reference electrode and 1M NaPF<sub>6</sub> (EC:PC) provided by E-lyte as electrolyte. The counter electrode has been different for positive or negative electrode characterization. AC positive electrodes are using an oversized activated carbon as counter electrode in order not to limit the fast adsorption/desorption mechanism of capacitive materials, whereas hard carbon negative electrodes are characterized using sodium metal as counter electrode to ensure sufficient sodium ions required to form a proper SEI and avoid electrolyte depletion.

In the case of the positive electrode, CVs between 2-4 V vs. Na<sup>+</sup>/Na have been carried out at different scan-rates between 10 to 100 mV s<sup>-1</sup> (see **Figure 17**). The butterfly and asymmetry shape of the CVs describes the difference size of the adsorbed solvated Na<sup>+</sup> and PF<sub>6</sub><sup>-</sup> ions. In the three studied cells, using different aluminium foils, it is observed that the rectangular shape is distorted with the increase of the scan-rate, what describes that the system is becoming more resistive. However, the tendency is very similar for the three studied aluminium foils (see **Figure 17a, 17b, 17c**), what does not make a difference when one of the aluminium foils must be selected. **Figure 17d** and **17e** compares all the systems at 20 mV s<sup>-1</sup> and 100 mV s<sup>-1</sup>, respectively, showing very close similarity.

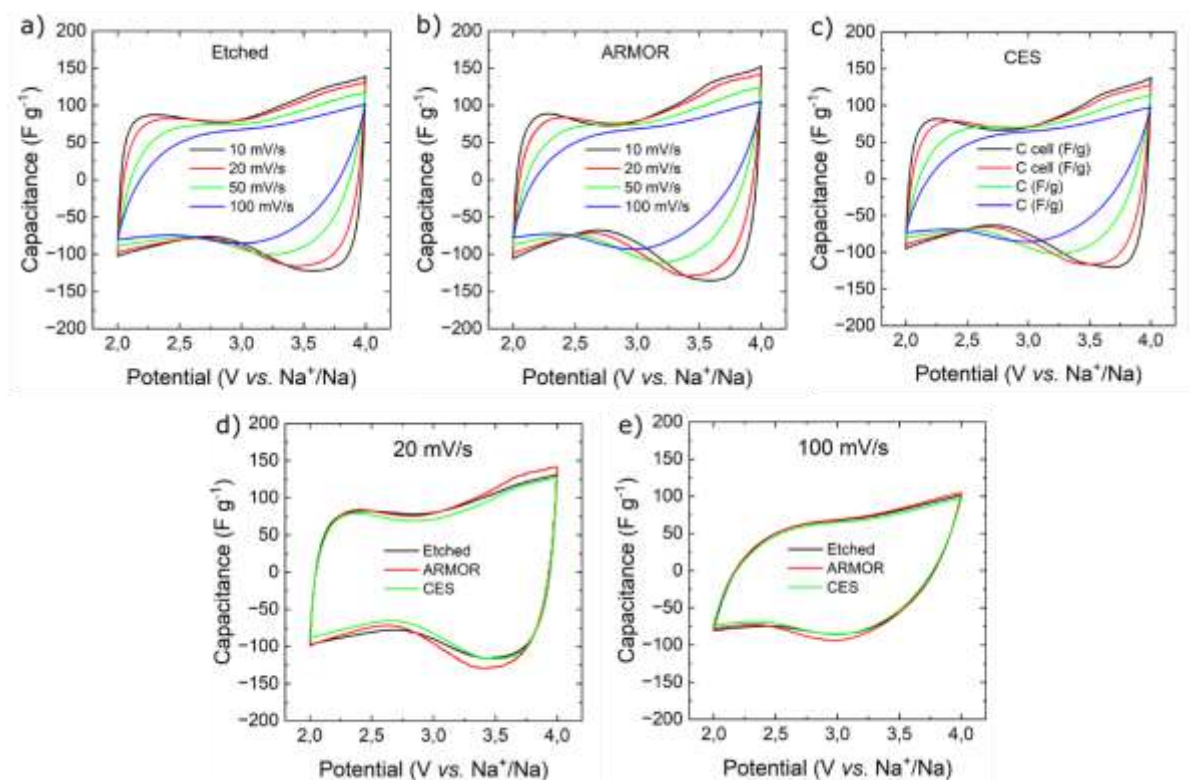


**Figure 17.** Cyclic voltammeteries for the positive electrodes fabricated in different aluminium foils: a) etched from Hohsen, b) carbon coated from ARMOR, c) carbon coated from CES, and comparison between them at d) 20 mV s<sup>-1</sup> and e) 100 mV s<sup>-1</sup>.

In terms of the galvanostatic charge/discharge measurements, **Figure 18a** shows that the capacitance values obtained with ARMOR-based electrodes are higher, while **Figure 18b** describes the charge/discharge profiles at 7 A g<sup>-1</sup>. If both graphs are analyzed, it can be concluded that the higher capacitance output of ARMOR-based electrodes might come from

the lower iR drop, but also due to some pseudocapacitive reactions that might have taken place. If the focus is set on the discharge profile of Figure 18b, some curvature can be observed for all the electrodes. However, it seems to be a little bit more pronounced for the ARMOR-based measurement. In order to be able to describe it to the current collector, more in-depth investigations would be needed.

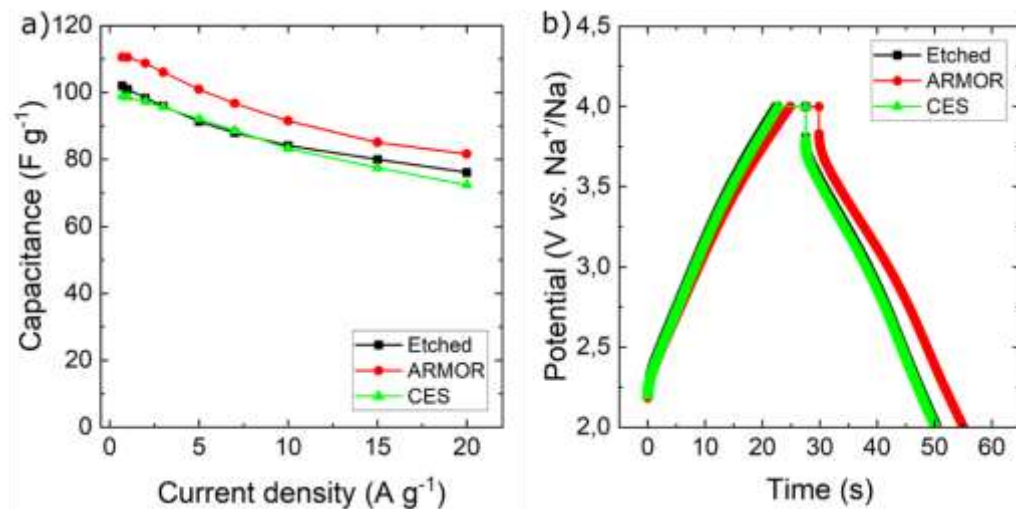


**Figure 18.** Galvanostatic charge/discharge measurements of the positive electrode with different aluminium foils: a) Specific capacitance output, and b) Profiles at 7 A g<sup>-1</sup>.

In the case of the negative electrode, CVs between 0.02-2 V vs. Na<sup>+</sup>/Na have been carried out at 1 mV s<sup>-1</sup> (see **Figure 19**). In this case, the purpose of the CV measurement is to evaluate the faradaic peaks of the HC material. The reduction curve of **Figure 19a** describes some small peaks in the range of 0.3-0.8 V vs. Na<sup>+</sup>/Na. These peaks describe the electrolyte decomposition and further SEI formation on the HC surface, while the lowest peak at 0.1 V vs. Na<sup>+</sup>/Na describes the insertion of Na<sup>+</sup> into the carbon layers. During the oxidation process, a unique peak corresponding to the deinsertion of Na<sup>+</sup> is described. **Figure 19b** describes the 10<sup>th</sup> cycle of the measurement, where sharper peaks are observed at the active potential of the HC.

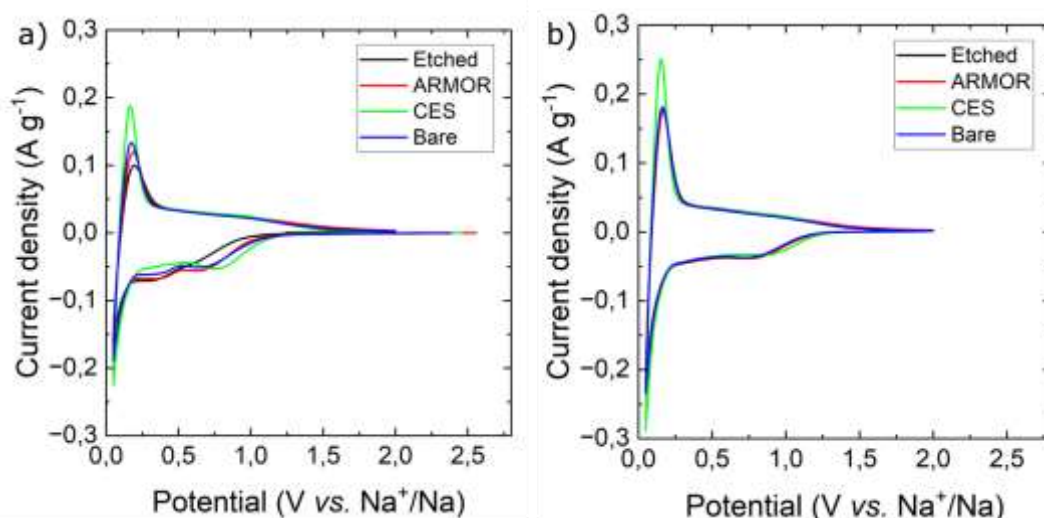


**Figure 19.** Cyclic voltammeteries for the negative electrodes fabricated in different aluminium foils: a) 1<sup>st</sup> cycle, and b) 10<sup>th</sup> cycle both at 1 mV s<sup>-1</sup>.



**Figure 20** describes the galvanostatic charge/discharge measurements. **Figure 20a** shows the first charge/discharge cycle of each of the electrodes, and **Figure 20b** the capacity output of them at different current densities. The profiles at Figure 20a show an initial sloppy profile during the charging step, where the SEI is created, while at around 100 mV vs. Na<sup>+</sup>/Na the insertion of Na<sup>+</sup> takes place. Initial coulombic efficiency of each electrode is 82.4% for etched, 82.0% for carbon coated ARMOR, 77.97% for carbon coating CES, and 74.71% for the bare aluminium foil. Even that values are quite similar, it should be highlighted the instable coulombic efficiency (CE) of the following cycles at same rate (i.e., 0.05 A g<sup>-1</sup>) in the case of HC electrodes made in bare or carbon coated CES aluminium foils. Meanwhile, the CE of the HC electrodes with etched or carbon coated ARMOR aluminium foils show much more stable CE in the first cycles. Rate capability measurements from Figure 20b reveal higher capacity output for bare and CES-based electrodes at low current densities. However, at higher rates, where the discharge time of interest is found, all electrodes are showing very similar performance. Thus, taking into consideration the first CE, and stability along the rate capability measurement, etched or carbon coated ARMOR based aluminium foils could be selected.

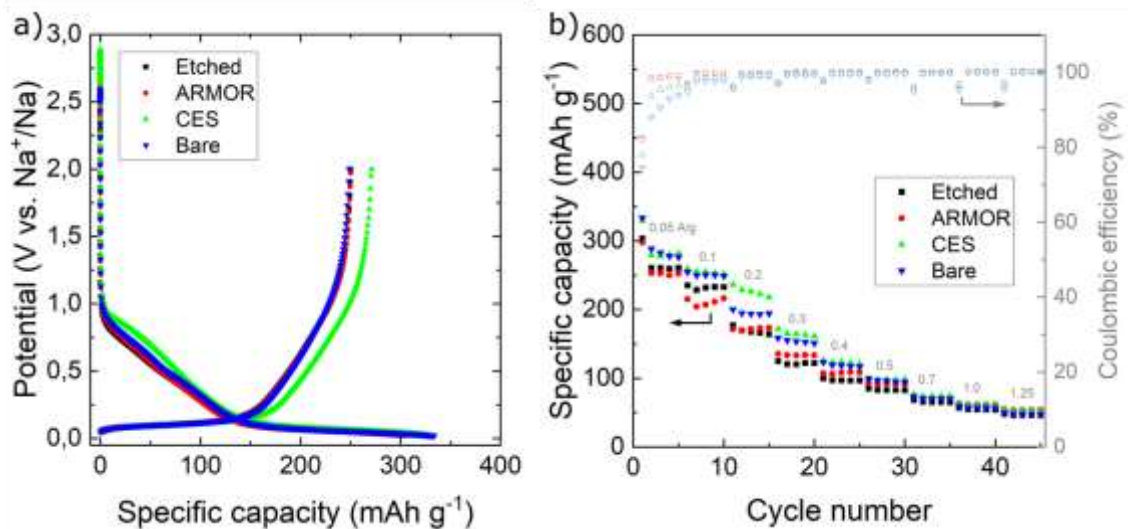


**Figure 20.** Galvanostatic charge discharge of the negative electrode in different current collectors: a) First charge/discharge profiles, and b) Rate capability.

### 3 Discussion and Conclusions

Gen0 materials have been selected as the baseline for the prototypes that are going to be developed in WP5, setting hard carbon and activated carbon as active materials, C45 as conductive additive and CMC or CMC:SBR as binders.

Disodium squarate has been selected as the Gen0 pre-sodiation agent and the most cost and performance effective squaric acid precursor has been selected for its synthesis, being this the one purchased by Apollo company. Moreover, a ratio of  $\text{Na}_2\text{C}_4\text{O}_4$ :C65 of 6:1 has been set to reduce the polarization and ensure the correct oxidation of the sacrificial salt.

In order to ensure good quality electrodes, different aluminium current collectors have been analysed for both AC-based and HC-based, positive and negative electrode, respectively. The formulation of the positive electrode has required to be adapted by introducing a rubberizer agent in order to avoid cracking and delamination at low mass loadings. The new CMC:SBR formulation has allowed to fabricate good quality electrodes with a mass loading of around  $3.7 \text{ mg cm}^{-2}$ . Meanwhile, HC electrodes have been fabricated with the initial formulation using only CMC as binder and allowing to work with electrodes of around  $2.5 \text{ mg cm}^{-2}$ .

Cross-sectional microstructural analysis and  $90^\circ$  adhesion tests have shown that AC electrodes present very good adhesion, while the cohesion might be improved; whereas HC electrodes might not show that excellent contact with the current collector, but the cohesion is excellent. However, physicochemical characterization does not clearly show which current collector might be the most appropriate one for each type of electrode, as all of them the show good properties.

With regard to the electrochemical characterization, on the one hand, positive electrodes show identical behaviour on CV measurements, while in the rate capability study, the ARMOR based electrodes show higher capacitance output. However, in this moment it cannot be concluded if that additional capacitance is related to the carbon coating of the current collector. On the other hand, the CV of negative electrodes show that CES electrodes are defining a sharper peak in the first cycle describing larger insertion of  $\text{Na}^+$ . However, rate capability measurements reveal that the sharper peak in the CV is describing also a lower initial coulombic efficiency, what it is not a desired scenario.

Overall, it is difficult to identify the best current collector for each electrode, since no significant evidence was observed, and some characterizations tip the balance to one side, and others to the other one. However, etched or carbon coated ARMOR aluminium foils for the positive electrode, and same ones for the negative electrode seem to be the most appropriate ones in terms of physicochemical and electrochemical characterization. However, other relevant parameters such as density, price, and origin of the component should be considered. Altogether, current collector from ARMOR company shows to be the most appropriate one. However, further aging analysis would be carried out in the following Task 5.2 and 5.3 to get a better conclusion about the most suitable aluminium foil.

## 4 Recommendation

More in-depth analysis is recommended to be able to select among etched and carbon coated ARMOR aluminium foils. Resistance evaluation by impedance measurements at pouch cell level might help to take this decision. Moreover, aging tests should be also carried out.

## 5 Risk register

**Table 4.** Risk Register

<b>Risk No.</b>	<b>What is the risk</b>	<b>Probability of risk occurrence<sup>1</sup></b>	<b>Effect of risk<sup>2</sup></b>	<b>Solutions to overcome the risk</b>
<b>WP5.1</b>	Supply problems with commercial materials (e.g., hard carbon, and activated carbon)	2-3	2-3	Check for alternative companies.
<b>WP5.2</b>	Parasitic reactions with carbon coated current collectors. (Section 2.3.4)	3	3	Bare aluminium foil would be utilized
<b>WP5.3</b>	Wrong decision on the selection of best current collector.	3	3	Ageing and impedance tests on Task 5.2 and 5.3 to double check.

<sup>1</sup> Probability risk will occur: 1 = high, 2 = medium, 3 = low

<sup>2</sup> Effect when risk occurs: 1 = high, 2 = medium, 3 = low

## 6 References

- [1] X. Dou, I. Hasa, D. Saurel, C. Vaalma, L. Wu, D. Buchholz, D. Bresser, S. Komaba, S. Passerini, Hard carbons for sodium-ion batteries: Structure, analysis, sustainability, and electrochemistry, *Materials Today*. 23 (2019) 87–104. <https://doi.org/10.1016/j.mattod.2018.12.040>.
- [2] D. Stępień, Z. Zhao, S. Dsoke, Shift to Post-Li-Ion Capacitors: Electrochemical Behavior of Activated Carbon Electrodes in Li-, Na- and K-Salt Containing Organic Electrolytes, *J. Electrochem. Soc.* 165 (2018) A2807. <https://doi.org/10.1149/2.0921811jes>.
- [3] G.G. Eshetu, G.A. Elia, M. Armand, M. Forsyth, S. Komaba, T. Rojo, S. Passerini, Electrolytes and Interphases in Sodium-Based Rechargeable Batteries: Recent Advances and Perspectives, *Advanced Energy Materials*. n/a (2020) 2000093. <https://doi.org/10.1002/aenm.202000093>.
- [4] M. Dahbi, T. Nakano, N. Yabuuchi, T. Ishikawa, K. Kubota, M. Fukunishi, S. Shibahara, J.-Y. Son, Y.-T. Cui, H. Oji, S. Komaba, Sodium carboxymethyl cellulose as a potential binder for hard-carbon negative electrodes in sodium-ion batteries, *Electrochemistry Communications*. 44 (2014) 66–69. <https://doi.org/10.1016/j.elecom.2014.04.014>.
- [5] N. Böckenfeld, S.S. Jeong, M. Winter, S. Passerini, A. Balducci, Natural, cheap and environmentally friendly binder for supercapacitors, *Journal of Power Sources*. 221 (2013) 14–20. <https://doi.org/10.1016/j.jpowsour.2012.07.076>.
- [6] D. Bhattacharjya, D. Carriazo, J. Ajuria, A. Villaverde, Study of electrode processing and cell assembly for the optimized performance of supercapacitor in pouch cell configuration, *Journal of Power Sources*. 439 (2019) 227106. <https://doi.org/10.1016/j.jpowsour.2019.227106>.
- [7] D. Bhattacharjya, M. Arnaiz, M. Canal-Rodríguez, S. Martin, T. Panja, D. Carriazo, A. Villaverde, J. Ajuria, Development of a Li-Ion Capacitor Pouch Cell Prototype by Means of a Low-Cost, Air-Stable, Solution Processable Fabrication Method, *Journal of The Electrochemical Society*. 168 (2021) 110544. <https://doi.org/10.1149/1945-7111/ac39e1>.
- [8] Anode Material for Lithium-ion Battery KURANODE™ BIOHARDCARBON | Kuraray. Activated Carbon Manufacturer, Anode Material for Lithium-Ion Battery KURANODE™ BIOHARDCARBON | Kuraray. Activated Carbon Manufacturer. (n.d.). <http://www.kuraray-c.co.jp/KURANODE/en.html> (accessed June 5, 2023).
- [9] Functional activated carbon | kuraray, (n.d.). <https://www.kuraray.com/products/kuraraycoal> (accessed June 5, 2023).
- [10] M. Arnaiz, D. Shanmukaraj, D. Carriazo, D. Bhattacharjya, A. Villaverde, M. Armand, J. Ajuria, A transversal low-cost pre-metallation strategy enabling ultrafast and stable metal ion capacitor technologies, *Energy Environ. Sci.* 13 (2020) 2441–2449. <https://doi.org/10.1039/D0EE00351D>.
- [11] C-ENERGY™ | Imerys, (n.d.). <https://www.imerys.com/product-ranges/c-nergy> (accessed June 5, 2023).

## 7 Acknowledgement

The author(s) would like to thank the partners in the project for their valuable comments on previous drafts and for performing the review.

**Table 5.** Project partners

#	PARTICIPANT SHORT NAME	PARTNER ORGANISATION NAME	COUNTRY
1	CICE	CENTRO DE INVESTIGACION COOPERATIVA DE ENERGIAS ALTERNATIVAS FUNDACION, CIC ENERGIGUNE FUNDAZIOA	Spain
2	EUR	CLANCY HAUSSLER RITA	Austria
3	KIT	KARLSRUHER INSTITUT FUER TECHNOLOGIE	Germany
4	CNRS	CENTRE NATIONAL DE LA RECHERCHE SCIENTIFIQUE CNRS	France
4.1	IMN	NANTES UNIVERSITE (Affiliated)	France
5	UPS	UNIVERSITE PAUL SABATIER TOULOUSE III	France
6	FSU	FRIEDRICH-SCHILLER-UNIVERSITAT JENA	Germany
7	IRT-JV	INSTITUT DE RECHERCHE TECHNOLOGIQUE JULES VERNE	France
8	ELY	E-LYTE INNOVATIONS GMBH	Germany
9	BYD	BEYONDER AS	Norway
10	BCARE	BATTERYCARE S. L.	Spain
11	TALGO	PATENTES TALGO SL	Spain



This project has received funding from the European Union's Horizon Europe programme for research and innovation under grant agreement No. 101092080.

This document reflects the views of the author and does not reflect the views of the European Commission. While every effort has been made to ensure the accuracy and completeness of this document, the European Commission cannot be held responsible for errors or omissions, whatever their cause.